Variational Monte Carlo Simulations for Elliptical and Spherical Bose Gas

Herman Brunborg, Elise Malmer Martinsen and Noémie Fritz
(Dated: March 28, 2022)

In this project we have studied the quantum mechanical properties of a Bose gas. We have computed the local energy of our gas in one, two and three dimensions for different numbers of particles using the Variational Monte Carlo method. For 100 particles in three dimensions in an elliptic trap, we obtained the expectation value of the local energy to be $\langle E_L \rangle = 241.4215 \pm 0.0036\hbar\omega_{\text{ho}}$ and $\langle E_L \rangle = 266.349 \pm 0.035\hbar\omega_{\text{ho}}$ with and without interactions between the particles, respectively. We found the optimal value of the variational parameter to be $\alpha = 0.500\text{m}^{-2}$ for the non-interactive case, while the α varies for the interactive case. With the Jastrow factor included, we could see an indication of the repulsive force between the bosons making them more spread out in the gas.

I. INTRODUCTION

A Bose gas is a gas consisting bosons which have integer spin. To study the gas on a microscopic level, we need to use quantum mechanical properties. In this paper we will study the ground state energy of a hard sphere Bose gas using Variational Monte Carlo (VMC) method and importance sampling based on the Fokker-Planck and Langevin equations. We have simulated a trap, containing a varying amount of particles, both as a spherical and elliptical harmonic trap in one, two and three dimensions.

Our goal is to find an optimal value for a variational parameter α used to compute the local energy of the Bose gas at a temperature $T = 0$K. The optimal variational parameter gives the lowest local energy of the system. We also want to investigate how the Bose gas spread out in space by calculating the onebody density of the gas.

One can study the model of the Bose gas for temperature $T = 0$K, and thereby discover important properties of the Bose-Einstein condensation, for example the critical temperature of the gas, the nature of the condensate and superfluidity [1].

In section II we explain the properties of our system, such as the Hamiltonian and the trial wave function. Furthermore, we consider the numerical aspects needed to study our system in section III. Here the Variational Monte Carlo method, the Metropolis algorithm, importance sampling, gradient method and the Blocking method are presented. In section IV and V we present and discuss our results, and in section VI we provide a short summary and outlook.

II. THEORY

A. The Hamiltonian and our trial wave function

To study the ground state energy of the system with N particles, we use either a spherical (S) or an elliptical (E) harmonic trap which is represented by an external potential V_{ext} given by

$$V_{\text{ext}}(\boldsymbol{r}) = \begin{cases} \frac{1}{2}m\omega_{\text{ho}}^2 r^2 & (S) \\ \frac{1}{2}m[\omega_{\text{ho}}^2(x^2+y^2)+\omega_z^2 z^2] & (E) \end{cases} \tag{1}$$

where m is the mass of a particle, ω_{ho} is a trap frequency in the xy-plane, $\boldsymbol{r}$ is the position of the particle, x, y and z are the coordinates of the particle and ω_{z} is the frequency in the z direction.

The Hamiltonian of the system is given by

$$H\Psi_T(\boldsymbol{r}) = \Big[\sum_{i=1}^{N}\Big(-\frac{\hbar^2}{2m}\nabla_i^2 + V_{ext}(\boldsymbol{r}_i)\Big) + \sum_{i<j}^{N} V_{int}(\boldsymbol{r}_i,\boldsymbol{r}_j)\Big]\Psi_T(\boldsymbol{r}) \tag{2}$$

where $\hbar$ is Plancks constant divided by 2π, V_{int} is a potential caused by the interactions between the particles given by

$$V_{\text{int}}(|\boldsymbol{r}_i - \boldsymbol{r}_j|) = \begin{cases} \infty & |\boldsymbol{r}_i - \boldsymbol{r}_j| \le a \\ 0 & |\boldsymbol{r}_i - \boldsymbol{r}_j| > a \end{cases} \tag{3}$$

and Ψ_{T} is our trial wave function given by

$$\Psi_T(\boldsymbol{r}) = \Psi_T(\boldsymbol{r}_1, \boldsymbol{r}_2, ..., \boldsymbol{r}_N, \alpha, \beta) \tag{4}$$

$$= \Big[\prod_i g(\alpha,\beta,\boldsymbol{r}_i)\Big]\Big[\prod_{j<k} f(a, |\boldsymbol{r}_j - \boldsymbol{r}_k|)\Big]. \tag{5}$$

Here, a is the hard-core diameter of the bosons, $g(\alpha,\beta,\boldsymbol{r}_i)$ is the single particle wave function given by

$$g(\alpha,\beta,\boldsymbol{r}_i) = \exp\{-\alpha(x_i^2 + y_i^2 + \beta z_i^2)\}. \tag{6}$$

For a spherical trap $\beta = 1$. $f(a, |\boldsymbol{r}_j - \boldsymbol{r}_k|)$, is the correlation wave function given by

$$f(a, |\boldsymbol{r}_i - \boldsymbol{r}_j|) = \begin{cases} 0 & |\boldsymbol{r}_i - \boldsymbol{r}_j| \le a \\ \Big(1 - \frac{a}{|\boldsymbol{r}_i - \boldsymbol{r}_j|}\Big) & |\boldsymbol{r}_i - \boldsymbol{r}_j| > a \end{cases} \tag{7}$$

For the non-interactive case we have $a = 0$, which means that $\alpha = 1/2a_{\text{ho}}^2$, where $a_{\text{ho}} = 1 - 2 \times 10^4$ Å. Since our system contains of bosons, our wave function needs to be symmetric under interchange of particles.

By introducing lengths in units of a_{ho}, i.e. $r \to r/a_{\text{ho}}$, we can rewrite our Hamiltonian as

$$H = \hbar\omega H' \tag{8}$$

where H' is a unitless Hamiltonian defined as

$$H' = \sum_{i=1}^{N} \frac{1}{2}\left(-\nabla_i^2 + x_i^2 + y_i^2 + \gamma^2 z_i^2\right) + \sum_{i<j} V_{\text{int}}(|\boldsymbol{r}_i - \boldsymbol{r}_j|) \tag{9}$$

where $\gamma = \omega_{\text{ho}}\omega_z^2$. Equation 8 leads to the following relation between the expectation values for the old and new Hamiltonians

$$\langle H\rangle = \hbar\omega\langle H'\rangle. \tag{10}$$

We will also need the drift force of the boson gas to be able to use Green's function, which we will apply in importance sampling as explained in section III. The drift force is given by

$$F = \frac{2\nabla\Psi_T}{\Psi_T} \tag{11}$$

It is possible to find an expression for the local energy and the drift force as shown in appendix B and C, respectively.

B. Variational Principle

To evaluate the ground state energy of the trapped Bose gas, we use the Variational principle, which is a very useful method since we find an upper limit for the ground state energy[2]. By taking an educated guess of an unnormalized trial wave function, Ψ_T, which depends on one or more variational parameters, we minimize the energy with respect to the variational parameters, and from this we find the lowest upper limit of the ground state energy E_{gs}. This is described in equation 12.

$$E_{gs} \leq \frac{\langle\Psi_T(\alpha)|H|\Psi_T(\alpha)\rangle}{\langle\Psi_T(\alpha)|\Psi_T(\alpha)\rangle} = \frac{\int \Psi_T^* H \Psi_T d\boldsymbol{r}}{\int \Psi_T^*\Psi_T d\boldsymbol{r}} \equiv \langle H\rangle, \tag{12}$$

where H is a known Hamiltonian of the system, and our trial wave function depends only on one variational parameter, α. $\langle H\rangle$ is the expectation value of H, which can be interpreted as the expectation value of the energy. If we already have a normalized wave function, we can rewrite equation 12 as

$$E_{gs} \leq \langle\Psi_T(\alpha)|H|\Psi_T(\alpha)\rangle = \int \Psi_T^* H \Psi_T d\boldsymbol{r} \equiv \langle H\rangle. \tag{13}$$

These statements are proven in Griffiths [2]. In Griffiths we can also see that the optimal value of the variational parameter α for one particle in one dimension is given by

$$\alpha = \frac{m\omega}{2\hbar} \tag{14}$$

This is found by setting the derivative of the expectation value of the Hamiltonian equal to zero

$$\frac{\partial\langle H\rangle}{\partial\alpha} = 0 \tag{15}$$

and solve with respect to α. In our simulation we will set $m\omega/\hbar = 1$, such that the optimal value for $\alpha = 0.5\text{m}^{-2}$. It is possible to generalize the expectation value of the Hamiltonian $\langle H_{ND}\rangle$ to N particles and D dimension by multiplying by the number of dimensions and particles as shown bellow.

$$\langle H_{ND}\rangle = ND\langle H_{11}\rangle. \tag{16}$$

Here $\langle H_{11}\rangle$ is the expectation of the Hamiltonian for one particle in one dimension. Since we find the optimal value for α by setting the derivative of $\langle H\rangle$ to zero, the optimal value will be the same no matter how many particles and dimensions we have.

III. METHOD

A. Variational Monte Carlo Method

The Variational Monte Carlo method applies the Variational principle, as explained in section II, to approximate the ground state energy numerically. For this, we need a probability distribution, which in our case will be described by our trial wave function, given in equation 4. We use Monte Carlo integration, which is a technique for numerically integration using random numbers, to evaluate the integral in equation 13.

In our model, the distribution of the next state, only depends on the current state. Therefore, the sequence of samples construct a Markov Chain that describes a sequence of probabilities of states. A Markov Chain is particularly suitable for this, as it works well for random systems with many uncertain variables [3]. Since we initialize the system randomly, the initial state might be an unlikely state. Therefore the first Monte Carlo cycles may give unlikely samples for the energy. Hence, we run 10% of the amount of cycles we wish to sample before we start to sample the energy of the system.

B. Metropolis algorithm

Since our system consists of bosons which have a symmetric wave function under interchange of particles, the probability distribution will also be symmetric. We can therefore use the Metropolis algorithm, which is a special case of the Metropolis Hastings algorithm. For each Monte Carlo cycle, we move one particle from an initial state, i, to a random position in a new state j with some transition probability $T_{i\to j}$. We then calculate the energy

in this position, and based on the probability distribution in state j, we either accept or deny the movement of the particle. If it is accepted we let the particle move to the new position with a acceptance probability $A_{i\to j}$. If it is denied, we let the particle stay in the same position as it was initially, with a probability $1 - A_{i\to j}$. We then update the average values, which in our case is the variance and the expectation value of the energy.

How we accept or deny the movement of the particle is based on maximizing the acceptance values,

$$A_{j\to i} = \min\left(1, \frac{p_i T_{i\to j}}{p_j T_{j\to i}}\right). \tag{17}$$

where p_i is our desired probability distribution that we obtain after running enough iterations. We use the pseudo random number generator Mersenne-Twister, with a period of $2^{19937} - 1$ [4], to generate random numbers that will contribute to either denying or accepting the movement of the particle. The Markov Chain Monte Carlo (MCMC) algorithm is shown in algorithm 1.

Algorithm 1 MCMC

- Start with current state x_i.
- Generate a new candidate x' using a proposal probability function distribution that only depends on x_i.
- Apply Metropolis rule:
- if accepted: $x_{i+1} = x'$
- if rejected: $x_{i+1} = x_i$
- Repeat

C. Importance Sampling

To get more efficient calculations, we replace the brute force Metropolis algorithm with importance sampling. Instead of having completely random walkers in our Monte Carlo simulations, we use walkers that are biased by the trial wave function. This method is based on the the Fokker-Planck and Langevin equations. We will partly show the relation between these equations. More information can be found in [5].

From the Langevin equation in one dimension, given by

$$\frac{\partial x(t)}{\partial t} = DF(x(t)) + \eta, \tag{18}$$

and using Euler's method, we can express the new position in coordinate space as

$$y = x + DF(x)\Delta t + \xi\sqrt{\Delta t}. \tag{19}$$

Here η is a random variable, Δt is a chosen time step, x is the previous position, ξ is a Gaussian random variable, and F_i is the i^{th} component of the drift force. The Fokker-Planck equation is given by

$$\frac{\partial P}{\partial t} = \sum_i D\frac{\partial}{\partial \boldsymbol{x_i}}\left(\frac{\partial}{\partial \boldsymbol{x_i}} - \boldsymbol{F_i}\right)P(\boldsymbol{x}, t) \tag{20}$$

where $P(\boldsymbol{x}, t)$ is the time-dependent probability density, and D is the diffusion coefficient. To obtain a stationary probability density, we set the left hand side of equation 20 equal to zero. From this equation we obtain the transition probability given by the Green's function

$$G(x, y, \Delta t) = \frac{1}{(4\pi D\Delta t)^{3N/2}}\exp\left\{-\frac{(y - x - D\Delta t F(x))^2}{4D\Delta t}\right\}. \tag{21}$$

The acceptance probability used in the Metropolis algorithm then becomes

$$A(y, x) = \min(1, q(y, x)) \tag{22}$$

where $q(y, x)$ now is defined by

$$q(y, x) = \frac{G(x, y, \Delta t)|\Psi_T(y)|^2}{G(y, x, \Delta t)|\Psi_T(x)|^2}. \tag{23}$$

D. Gradient Methods

The aim of this part is to find an optimal value of our variational paramter α using few Monte Carlo cycles. This optimal value, which will give the lowest upper limit of the ground state energy, will then be used in a full scale Monte Carlo simulation.

To do this we use the Gradient Descent algorithm. We start by initializing the variational parameter to a value α_0 and calculate the gradient of the expectation value of the energy $\langle E(\alpha)\rangle$ with respect to α. For each step we correct the value of α, subtracting by the gradient of the expectation value of the energy which again is multiplied by a learning rate, γ. This is shown in equation 24.

$$\alpha_{k+1} = \alpha_k - \gamma_k \nabla\langle E(\alpha_k)\rangle, \quad k \geq 0, \tag{24}$$

where α_{k+1} and α_k is respectively the new and old value of α. This is repeated until the value of α converges and we have reached the optimal value of α.

E. Blocking method

Our numerical experiment will have two classes of errors; statistical and systematical errors. The statistical errors can be estimated using statistical analysis, while the systematic errors are method specific and they are therefore different for each case.

To find the uncertainty of our simulation we use the Blocking method. We use this method instead of other

resampling methods, such as Bootstrapping, since the Blocking method is more efficient for large sets of data [6], $n > 10^5 \sim 10^6$, where n is the number of data points. Using the Blocking method, we transform our data set X, with n data points, into data set X' given in equation 25 and 26, respectively.

$$X = x_1, x_2, ..., x_n \tag{25}$$

$$X' = [x'_1, x'_2, ..., x'_{n'}], \quad n' = \frac{1}{2}n \tag{26}$$

The new data points, given in equation 27, is collected into blocks containing half as large data sets without loosing any data. We do this by computing the mean of the neighbouring data points, which is why no data is lost. Therefore, we will still end up with the same mean value and variance.

$$x'_i = \frac{1}{2}[x_{2i-1} + x_{2i}]. \tag{27}$$

We divide our data set into m experiments with n data points in each experiment. The total variance σ^2 of all the data points is given by

$$\sigma^2 = \frac{1}{mn}\sum_i (x_i - \mu)^2. \tag{28}$$

The variance σ_m^2 of an experiment m is given by

$$\sigma_m^2 = \frac{\sigma^2}{n} + \text{COV} \tag{29}$$

where COV is the covariance given by

$$\text{COV}(X) = \frac{1}{n}\sum_k \sum_l (x_k - \bar{x}_n)(x_l - \bar{x}_n). \tag{30}$$

This is a double sum which is computationally heavy. We therefore want to find a way to compute the variance of the experiment m without having to compute the covariance.

We can define f_d, which describes the correlation between measurements separated by the distance d in the samples, as

$$f_d = \frac{1}{n-d}\sum_{k=1}^{n-d}(x_k - \bar{x}_n)(x_{k+d} - \bar{x}_n). \tag{31}$$

The autocorrelation function κ_d, which describes the pairwise correlations, is then given by

$$\kappa_d = \frac{f_d}{\sigma^2}. \tag{32}$$

If we divide our data set into enough blocks we will eventually get smaller data sets that are not correlated. The truncation error is given by

$$e_k = \frac{2}{n_k}\sum_{h=1}^{n_k-1}\left(1 - \frac{h}{n_k}\right)\gamma_k(h) \tag{33}$$

where γ_k is the autocovariance which is the normalized autocorrelation κ_k. If we apply the Blocking method enough times the autocovariance will eventually get so small that we can estimate the variance as

$$\sigma_m^2 = \frac{\sigma_k^2}{n} + e_k, \quad 0 \le k \le d-1 \tag{34}$$

$$\approx \frac{\sigma_k^2}{n} \tag{35}$$

where k is the number of blocking transformations and σ_k is the variance at a specific blocking iteration. This is the equation we will implement in our simulation. The proofs of this method is given in [6].

F. Parallelizing our code

Our Monte Carlo simulation is computationally heavy. We will therefore parallelize our code to make it more efficient. Since we are running a lot of different systems, while each system runs independently of the other systems we simulate, we use OpenMP. Since we do not communicate between the threads, adding another thread will lead to an increase of nearly as much as the speed of the thread itself, since we will have very little overhead.

G. Jastrow Factor

Because of the interactive force between the bosons, we include a Jastrow factor in the trial wave function as shown in equation 4. This factor makes sure that the bosons are not overlapping and spreads the particles apart. The Jastrow factor is described as shown in equation 7.

H. Onebody Densities

Onebody density is a way to find the spacial distribution of the particles in the hard sphere Bose gas. This is described by

$$\rho(\boldsymbol{r}) = N\int d\boldsymbol{r_2}d\boldsymbol{r_3}...d\boldsymbol{r_N}|\Psi_T(\boldsymbol{r_1}, \boldsymbol{r_2}, ..., \boldsymbol{r_N})|^2 \tag{36}$$

where N is the number of particles. This integral is implemented in our simulation by making histograms with the position on the x-axis and the density on the y-axis, and we check how many particles are present, or have passed through each block in the histogram.

If we have repulsive interactions between the particles, the onebody density will have a wider distribution than bosons with no interactions. For the attractive case, on the other hand, the onebody density will be narrower.

One can therefore use the onebody density to find out if the particles in a gas repulse or attract each other. The onebody density can also be used to find out how strong the forces between the particles are.

IV. RESULTS

Figure 1 shows the acceptance rate for the brute force metropolis algorithm and the importance sampling as a function of step length Δt for both the interactive and non-interactive case. Figure 14, 2 and 3 shows the energy as a function of the variational parameter, α, for 10, 50 and 100 particles with interactions in three dimensions, respectively.

Figure 15, 16 and 4 show the energy as a function of the variational parameter, α, for 1 particle without interactions in one, two and three dimension, respectively, for analytical and numerical brute force and importance sampling.

In figure 17, 18 and 5, the energy is presented as a function of the variational parameter, α, for 10 particles without interactions in one, two and three dimension, respectively, for analytical and numerical brute force and importance sampling.

Figure 19, 20 and 6 show the energy as a function of the variational parameter, α, for 100 particles without interactions in one, two and three dimension, respectively, for analytical and numerical brute force and importance sampling.

We have also presented the energy as a function of the variational parameter, α, for 500 particles without interactions in one, two and three dimension, respectively, for analytical and numerical brute force and importance sampling. This is shown in figure 21, 22 and 7.

Figure 8 and 9 show the gradient descent steps for different values of the variational parameter α as a function of iterations with and without interactions, respectively. Without interactions the optimal value for $\alpha = 0.5000/\mathrm{m}^2$, while with interactions the optimal value of our variational parameter was estimated to different values depending on the number of particles. The dotted line shows the estimated alpha values.

The CPU-time for numerical and analytical brute force Metropolis calculations for different number of particles and dimensions is presented in figure 10.

Tables I and II shows expectation value of the local energy, the standard deviation and the CPU-time for increasing number of particles with and without interactions.

The plots of the onebody density for 10, 50 and 100 particles are presented in figure 11, 12 and 13, respectively.

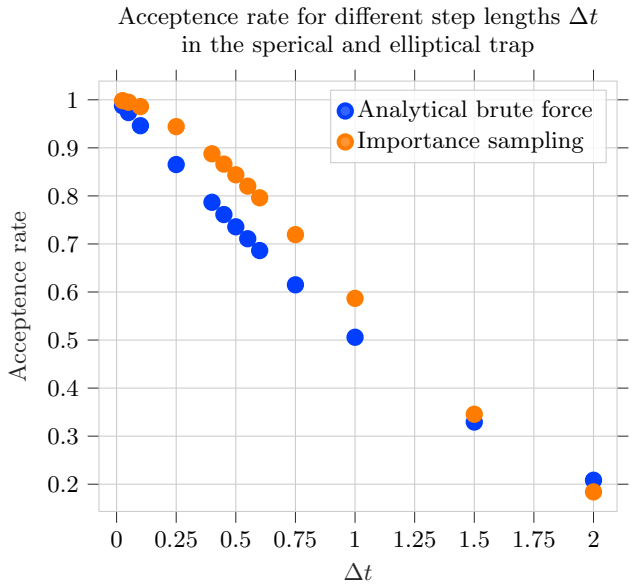

Figure 1. Acceptance rate for the brute force metropolis algorithm and the importance sampling as function of step length Δt.

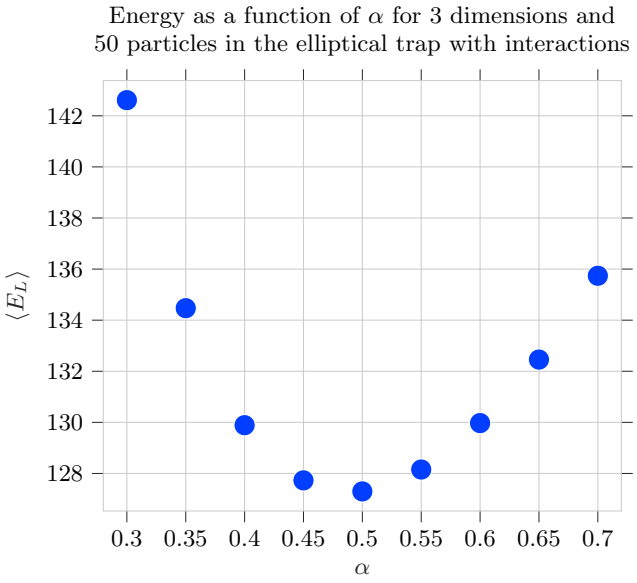

Figure 2. Energy as a function of the variational parameter α for 50 particles with interactions in 3 dimensions.

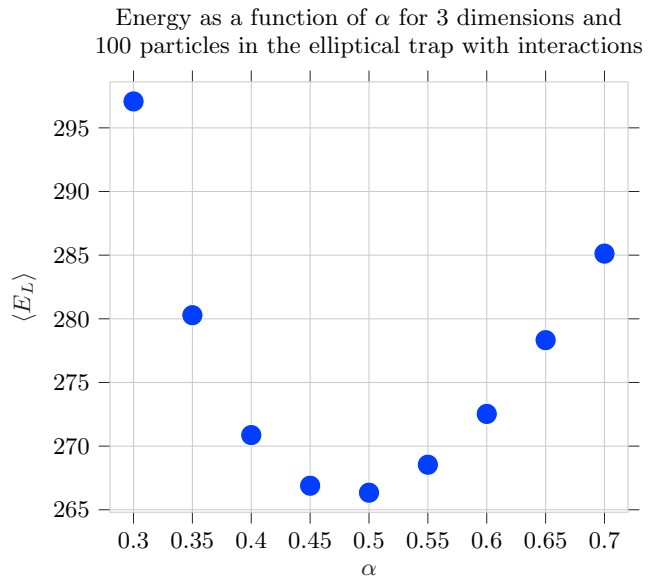

Figure 3. Energy as a function of the variational parameter α for 100 particles with interactions in 3 dimensions.

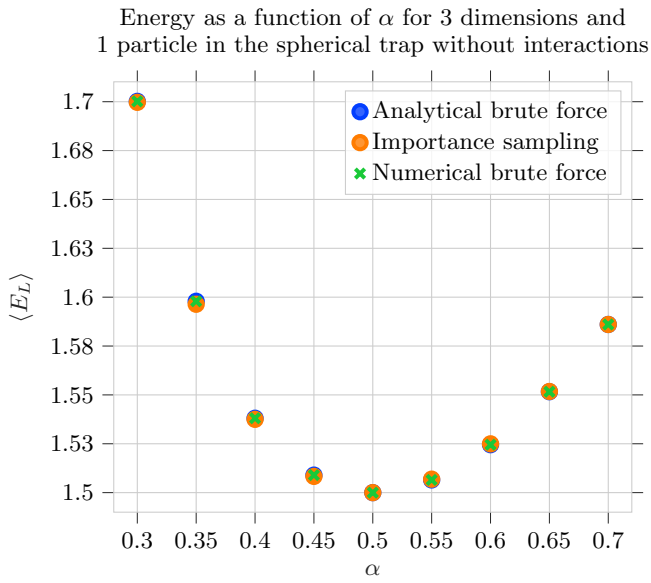

Figure 4. Energy as a function of the variational parameter, α, for 1 particle without interactions in 3 dimensions, for analytical and numerical brute force and importance sampling.

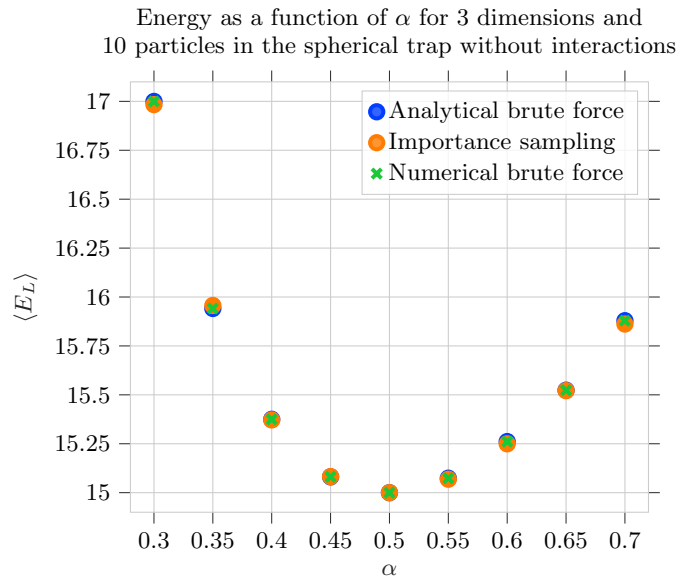

Figure 5. Energy as a function of the variational parameter, α, for 10 particles without interactions in 3 dimensions, for analytical and numerical brute force and importance sampling.

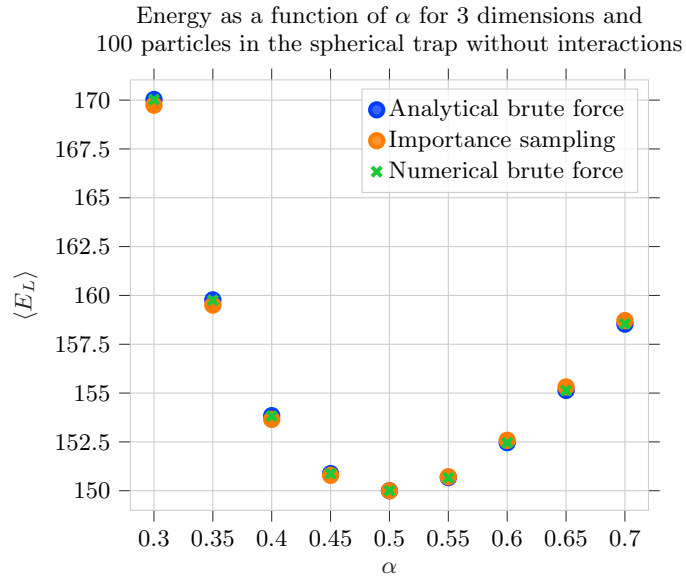

Figure 6. Energy as a function of the variational parameter, α, for 100 particles without interactions in 3 dimensions, for analytical and numerical brute force and importance sampling.

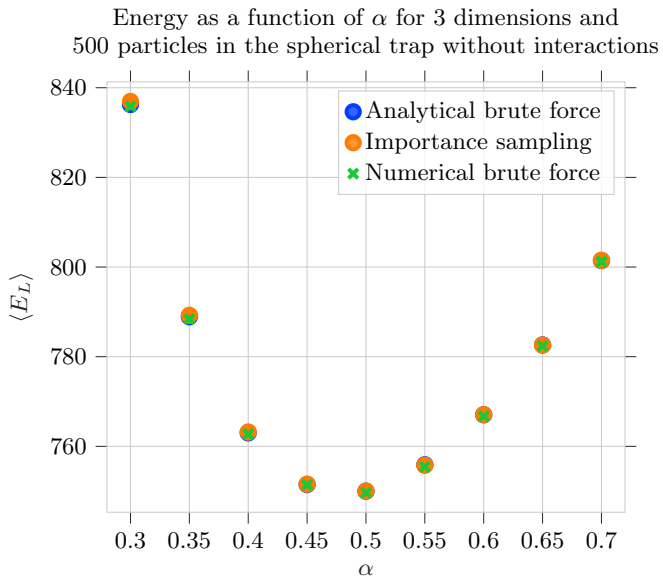

Figure 7. Energy as a function of the variational parameter, α, for 500 particles without interactions in 3 dimensions, for analytical and numerical brute force and importance sampling.

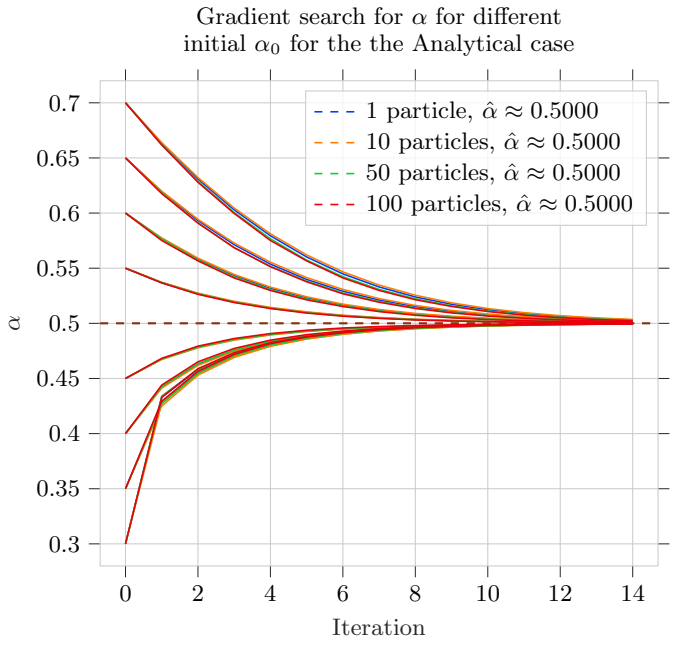

Figure 8. Gradient descent showing the variational parameter α as a function of iterations for different start values of α, without interactions and for 10 particles. The learning rate, η, is $5 \cdot 10^{-2}/N$.

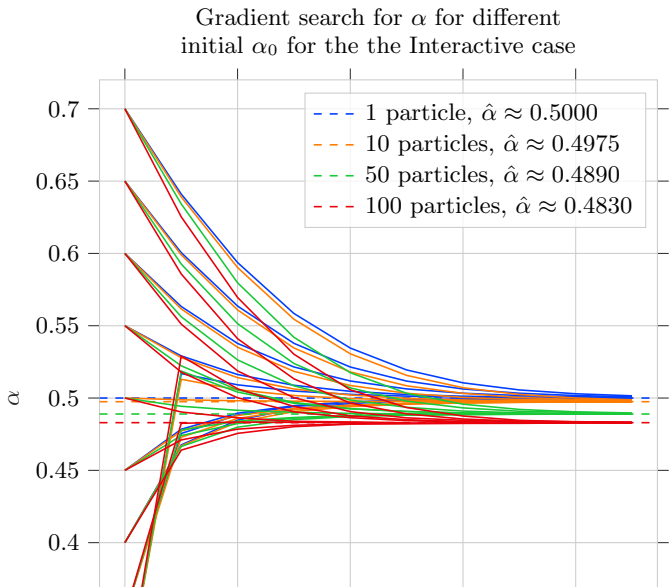

Figure 9. Gradient descent showing the variational parameter α as a function of iterations for different start values of α, with interactions and for 10 particles.The learning rate, η, is $5 \cdot 10^{-2}/N$.

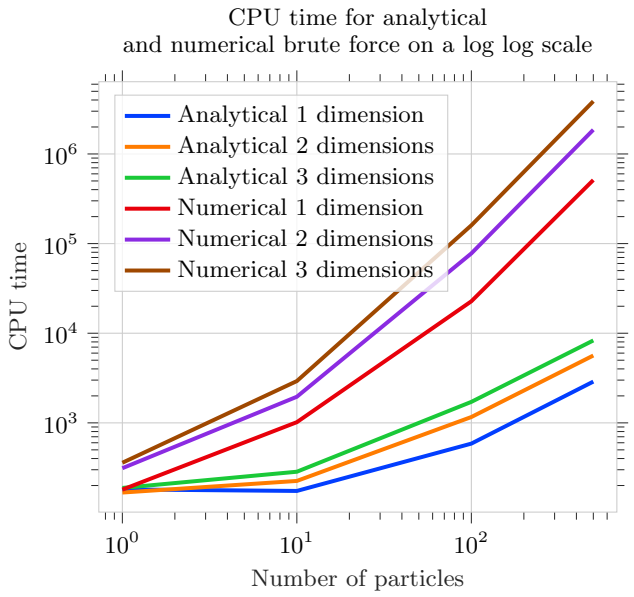

Figure 10. Figure showing the CPU-time for numerical and analytical brute force Metropolis calculations for different number of particles and dimensions.

Table I. The expectation values of the local energy in an elliptical trap with corresponding standard error for different numbers of particles, N, in three dimensions without interactions and the CPU-time for the simulations.

N	$\langle E_L\rangle[\hbar\omega_{\text{ho}}]$	σ_{block}	Time[s]	$\langle E_L\rangle/N[\hbar\omega_{\text{ho}}]$
10	24.14213	0.00039	2.346	2.414213
50	120.7107	0.0018	29.903	2.414214
100	241.4215	0.0036	116.510	2.414215

Table II. The expectation values of the local energy in an elliptical trap with corresponding standard error for different numbers of particles, N, in three dimensions with interactions and the CPU-time for the simulations.

N	$\langle E_L\rangle[\hbar\omega_{\text{ho}}]$	σ_{block}	Time[s]	$\langle E_L\rangle/N[\hbar\omega_{\text{ho}}]$
10	24.3982	0.00045	1.431	2.43982
50	127.299	0.011	2.346	2.54598
100	266.349	0.035	126.345	2.66349

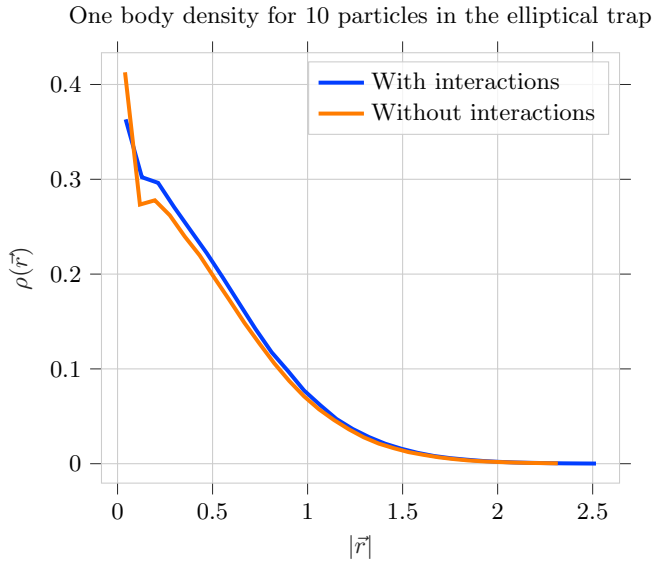

Figure 11. Onebody density for 10 particles in three dimensions with and without interactions.

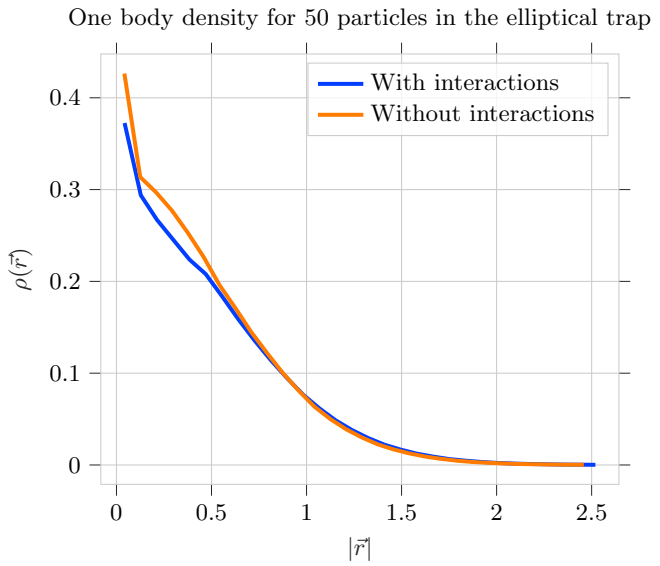

Figure 12. Onebody density for 50 particles in three dimensions with and without interactions.

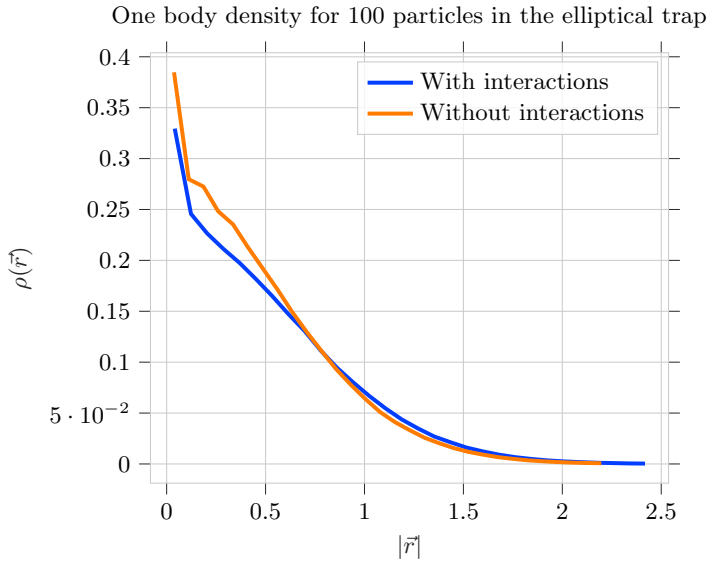

Figure 13. Onebody density for 100 particles in three dimensions with and without interactions.

V. DISCUSSION

A. Choosing Δt

In figure 1 we see as expected, that the lower Δt, the higher acceptance rate we obtain. This happens because we take a smaller step, and the difference in the energy before and after taking the step will also be smaller. Thus, the acceptance rate will increase.

When we run the metropolis steps, we want to explore the entire domain, while still being efficient. This means that we want to spend more cycles in likely states. This means that our step length must be big enough so that we move to the likely states. Therefore, we do not want our acceptance rate to be too high, as this would mean that we accept also unlikely steps, and that we will move slowly toward the more likely states. On the other hand, we also do not want it too low, as this would mean that we do a lot of computations without actually evolving our system. Therefore it is desired to have an acceptance rate around $60\% - 80\%$. From figure 1 we see that $\Delta t = 0.5$s gives an acceptance rate within this range for the brute force Metropolis algorithm, and we therefore use this as our Δt.

When we run the importance sampling, we utilize the drift force to make steps in more likely directions. This allows us to run the importance sampling with a higher acceptance rate, as compared to the brute force method. From figure 1 we see that the acceptance rate is slightly higher. It would also be possible to use an even higher acceptance rate, but for simplicity, we used the same Δt as for the brute force method.

B. Finding the optimal value for our variational parameter

From figures 5, 6, 21, and 7, and the plots concerning the non-interactive plots in appendix E we see that for all the spherical systems without interactions, we obtain the lowest energy when $\alpha = 0.5\text{m}^{-2}$. This is as expected as we wrote in II B.

Figures 2 and 3 and the plots concerning the interactive plots in appendix E show that the optimal value for α diverges from 0.5m^{-2}. This is as expected since the Hamiltonian, which decides the energy of the system, changes when we include interactions between the bosons.

In figure 8, we can see that no matter what our initial value of α is, the gradient descent method finds our optimal value of α to be approximately 0.5m^{-2}. For the case without interactions, this corresponds well with our analytical value for the optimal α.

For the gradient search with interactions, which can be seen in figure 9, we see that we find different estimates for α for the different number of particles. For the case with one particle, we will not get any interactions, which explains why we get the same value as for the non-interactive case. For the other number of particles, we see that the more particles we have, the more it deviates from 0.5. This also makes sense, since more particles will mean more interactions.

C. CPU-time

Figure 10 shows that the CPU-time for the numerical calculations for the derivatives take significantly longer time than the analytical calculations, as expected. This is caused by the numerical calculations that need to move and evaluate the positions for each particle and dimension and evaluate the particle for each of these, while the analytical only need to evaluate the particle once. This also means that the numerical case will be slower and slower compared to the analytical, the more particles we include. This is also what we observe from the plot.

D. Blocking method

From table I and II we see that the expectation value of the local energy increases with the number of particles, which is as expected. According to equation 16, we see that the expectation value of the energy is proportional to the number of particles for the non-interacting case. No matter how many particles there are in the gas, we will have the same ratio, $2.414\hbar\omega_{\text{ho}}$, between the local energy and the number of particles. Thus, $\langle E_L \rangle$ increases with the number of particles for the non interacting case. However, for the interacting case in table II we see the same tendency, but the local energy per particle increases with the number of particles. We see for table II that we get different values for the estimated optimal variational paramter, $\hat{\alpha}$, when we include interactions. This might be caused by the number of particles effecting the interactive potential. Hence, it does not seem unlikely that the optimal value of $\hat{\alpha}$ will vary as a consequence of this.

We also observe that the relative standard deviation has the same magnitude of 10^{-5}, except for the case with 100 particles in table II, which has a magnitude of 10^{-4}. This is a very small standard error, which indicates that our simulations are precise.

E. Onebody density

From figure 12 and 13 we can see that the graph for the onebody density indicates that the bosons are more spread in the gas with interactions, i.e. Jastrow factor included, than without interactions. This is as expected since bosons repulse from each other. Since the bosons now are more spread, the radius of the sphere will increase and therefore the density for small radii will decrease. Without interactions, the bosons will not be affected by each other, hence, the onebody density in this case will have larger values for lower radii.

Figure 11 on the other hand, shows that the onebody density is higher for the gas with interactions than for the gas without interactions for small radii. This is not

as expected and might be explained by the small number of particles and randomness. We also remember that in the case with 10 particles from Figure 9, the estimated α was very close to 0.5.

VI. CONCLUSION

To summarize, we have studied the local energy of bosons in both a spherical and an elliptical trap using the Variational Monte Carlo method. The expectation values of the local energies without interactions were found to be $24.14213 \pm 0.00039\hbar\omega_{\text{ho}}$, $120.7207 \pm 0.0018\hbar\omega_{\text{ho}}$ and $241.4215 \pm 0.0036\hbar\omega_{\text{ho}}$ for 10, 50 and 100 particles, respectively, in an elliptical trap. Including the interactions, we obtain the expectation values of the local energies to be $24.3982 \pm 0.00045\hbar\omega_{\text{ho}}$, $127.299 \pm 0.011\hbar\omega_{\text{ho}}$ and $266.349 \pm 0.035\hbar\omega_{\text{ho}}$ for 10, 50 and 100 particles, respectively, in an elliptical trap.

We obtained the value for the variational parameter using the gradient method, and it was found to be 0.5000m^{-2} without the Jastrow factor for the spherical trap, and varying from 0.5000 to 0.4829 with the Jastrow factor for the elliptical trap. Including the Jastrow factor, we saw the repulsive tendency of the bosons making them spread more in the gas, which gives a smaller onebody density for lower radii. In the simulations we chose $\Delta t = 0.5\text{s}$ to obtain the desired acceptance rate. As expected, we saw that the CPU-time for the numerical calculations is significantly longer than the analytical calculations of the derivatives.

For further studies one can replace the bosons with fermions and see how the Pauli exclusion principle affect the expectation values of the energy. Another proposal for further work is making the code more efficient. The non-linear time complexity of our current code for calculating local energy for the elliptical case per Monte Carlo cycle, can be improved since we move only one particle at the time. We could cache all the calculations which remain the same, making the code run in linear time per cycle. This will allow running simulations with a greater amount of particles in a more reasonable time frame.

ACKNOWLEDGMENTS

We would like to thank Øyvind Sigmundson Schøyen for answering all of the 10^{∞} questions we asked each group session.

REFERENCES

[1] S. Perkowitz. *Bose-Einstein condensate*. URL: https://www.britannica.com/science/Bose-Einstein-condensate.

[2] Schroeter D. F. Griffiths D. J. *Quantum Mechanics*. One Liberty Plaza, 20th Floor, New York, NY 10006, USA: Cambridge Univesity Press, 2018.

[3] *Markov Chain*. Accessed 25.03.22. URL: https://www.sciencedirect.com/topics/social-sciences/markov-chain.

[4] William J Buchanan. *Mersenne Twister*. Accessed 25.03.22. URL: https://asecuritysite.com/encryption/twister.

[5] N. G. Van Kampen. *Stochastic Processes in Physics and Chemistry*. Institute for Theoretical Physics of the University at Utrecht: Springer, 2007.

[6] M. Jonsson. *Standard error estimation by an automated blocking method*. Accessed 25.03.22. URL: https://journals.aps.org/pre/pdf/10.1103/PhysRevE.98.043304.

Appendix A: Source code

Our code can be found here: https://github.com/elisemma/FYS4411/tree/main/project1

Appendix B: Analytic expression for local energy neglecting two-body potential

It is possible to find an analytic expression for the local energy, $E_L(\boldsymbol{r})$, for the trial wave function, $\Psi_T(\boldsymbol{r})$, given in equation 4. To do this, we start by finding the local energy in the case with only the harmonic oscillator potential, so that $a = 0$ and we neglect the two-body potential.

The local energy is given by

$$E_L(\boldsymbol{r}) = \frac{1}{\Psi_T(\boldsymbol{r})} H\Psi_T(\boldsymbol{r}), \tag{B1}$$

where the Hamiltonian, H, is given in equation 2. For simplicity, we start by letting the Hamiltonian act on our trial wave function,

$$H\Psi_T(\boldsymbol{r}) = \Big[\sum_{i=1}^{N}\Big(-\frac{\hbar^2}{2m}\nabla_i^2 + V_{ext}(\boldsymbol{r}_i)\Big) + \sum_{i<j}^{N} V_{int}(\boldsymbol{r}_i, \boldsymbol{r}_j)\Big]\Psi_T(\boldsymbol{r}) \tag{B2}$$

We see that the Laplace operator is the only thing that will change the trial wave function. Therefore we let the Laplace operator act on the trial wave function,

$$\nabla_i^2\Psi_T(\boldsymbol{r}) = \Big(\frac{\partial^2}{\partial x_i^2} + \frac{\partial^2}{\partial y_i^2} + \frac{\partial^2}{\partial z_i^2}\Big)\Psi_T(\boldsymbol{r}) = 4\alpha^2(x_i^2 + y_i^2 + \beta^2 z_i^2) - 4\alpha - 2\alpha\beta.$$

Since we are going to find the local energy in the case with only the harmonic oscillator potential, the Hamiltonian acting on the trial wave function becomes,

$$\Psi_T(\boldsymbol{r}) = \sum_{i=1}^{N}\Big[-\frac{\hbar^2}{2m}(4\alpha^2(x_i^2 + y_i^2 + \beta^2 z_i^2) - 4\alpha - 2\alpha\beta) + \frac{1}{2}m\omega_{\text{ho}}^2(x_i^2 + y_i^2 + z_i^2)\Big]\Psi_T(\boldsymbol{r}) \tag{B3}$$

We are going to use $\beta = 1$ since we look at the case with a spherical trap, so the analytic expression for the local energy is given by

$$E_L(\boldsymbol{r}) = \sum_{i=1}^{N}\Big(-\frac{\hbar^2}{2m}(4\alpha^2 r_i^2 - 6\alpha) + \frac{1}{2}m\omega_{\text{ho}}^2 r_i^2\Big) \tag{B4}$$

Appendix C: Analytic exrpession for drift force

For the importance sampling, we need the drift force which is given as shown in equation 11. Also here we consider only the harmonic oscillator part with a spherical trap, so $\beta = 1$. We start by computing $\nabla\Psi_T(\boldsymbol{r})$, which gives us

$$\nabla\Psi_T(\boldsymbol{r}) = \sum_{i=1}^{N}\nabla_i\Psi_T(\boldsymbol{r}) = \sum_{i=1}^{N} -2\alpha(x_i + y_i + \beta z_i)\Psi_T(\boldsymbol{r}). \tag{C1}$$

The drift force is then given by

$$F = -4\alpha\sum_{i=1}^{N}(x_i + y_i + \beta z_i). \tag{C2}$$

Appendix D: Analytic expression for local energy including interaction between the bosons

To be able to find the analytic expression for the local energy including the interaction between the bosons, i.e. $a \neq 0$, we need to rewrite the trial wave function as

$$\Psi_T(\boldsymbol{r}) = \Big[\prod_i g(\alpha, \beta, \boldsymbol{r}_i)\Big] \exp\Big\{\sum_{i<k} u(r_{jk})\Big\}, \tag{D1}$$

where $u(r_{ij}) = \ln f(r_{ij})$. We need to compute

$$\frac{1}{\Psi_T(\boldsymbol{r})} \sum_i^N \nabla_i^2 \Psi_T(\boldsymbol{r}). \tag{D2}$$

We start by finding the first derivative for particle k:

$$\nabla_k \Psi_T(\boldsymbol{r}) = \nabla_k \Big[\prod_i \phi(\boldsymbol{r}_i)\Big] \exp\Big\{\sum_{j<k} u(r_{jk})\Big\}, \tag{D3}$$

where we have defined that $r_{jk} = |\boldsymbol{r}_j - \boldsymbol{r}_k|$. Using the Product Rule, we obtain

$$\nabla_k \Psi_T(\boldsymbol{r}) = \nabla_k \Big[\prod_k \phi(\boldsymbol{r}_k)\Big] \exp\Big\{\sum_{j<m} u(r_{jm})\Big\} + \Big[\prod_i \phi(\boldsymbol{r}_i)\Big] \nabla_k \exp\Big\{\sum_{j<m} u(r_{jm})\Big\}.$$

Now, using the Chain Rule we obtain

$$\nabla_k \Psi_T(\boldsymbol{r}) = \nabla_k \phi(\boldsymbol{r}_k) \Big[\prod_{i\neq k} \phi(\boldsymbol{r}_i)\Big] \exp\Big\{\sum_{j<m} u(r_{jm})\Big\} + \Big[\prod_i \phi(\boldsymbol{r}_i)\Big] \exp\Big\{\sum_{j<m} u(r_{jm})\Big\} \sum_{l\neq k} \nabla_k u(r_{kl}).$$

We now need to find the second derivative of the trial wave function. Therefore we simply find the derivative of the expression we just found given in equation D4. Using both the Product Rule and the Chain Rule we then obtain

$$\nabla_k^2 \Psi_T(\boldsymbol{r}) = \Big[\nabla_k^2 \phi(\boldsymbol{r}_k) \exp\Big\{\sum_{j<m} u(r_{jm})\Big\} \tag{D4}$$

$$+ \nabla_k \phi(\boldsymbol{r}_k) \exp\Big\{\sum_{j<m} u(r_{jm})\Big\} \sum_{l\neq k} \nabla_k u(r_{kl})\Big] \Big(\prod_{i\neq k} \phi(\boldsymbol{r}_i)\Big) \tag{D5}$$

$$+ \nabla_k \phi(\boldsymbol{r}_k) \Big[\prod_{i\neq k} \phi(\boldsymbol{r}_i)\Big] \exp\Big\{\sum_{j<m} u(r_{jm})\Big\} \sum_{l\neq k} \nabla_k u(r_{kl}) \tag{D6}$$

$$+ \Big[\prod_i \phi(\boldsymbol{r}_i)\Big] \exp\Big\{\sum_{j<m} u(r_{jm})\Big\} \sum_{l\neq k} \nabla_k^2 u(r_{kl}) \tag{D7}$$

Now, we multiply by $\phi(\boldsymbol{r}_k)/\phi(\boldsymbol{r}_k)$ and factorize. We obtain

$$\nabla_k^2 \Psi_T(\boldsymbol{r}) = \Big[\frac{\nabla_k^2 \phi(\boldsymbol{r}_k)}{\phi(\boldsymbol{r}_k)} + \frac{2\nabla_k \phi(\boldsymbol{r}_k)}{\phi(\boldsymbol{r}_k)} \sum_{l\neq k} \nabla_k u(r_{kl}) + \sum_{l\neq k} \nabla_k^2 u(r_{kl}) + \sum_{l\neq k} \sum_{n\neq k} \nabla_k u(r_{kl}) \nabla u(r_{kn})\Big] \Psi_T(\boldsymbol{r}). \tag{D8}$$

Computing the derivatives of $u(r_{kl})$, we obtain

$$\frac{1}{\Psi_T(\boldsymbol{r})}\nabla_k^2\Psi_T(\boldsymbol{r}) = \frac{\nabla_k^2\phi(\boldsymbol{r}_k)}{\phi(\boldsymbol{r}_k)} + \frac{2\nabla_k\phi(\boldsymbol{r}_k)}{\phi(\boldsymbol{r}_k)}\left(\sum_{l\neq k}\frac{(\boldsymbol{r}_k-\boldsymbol{r}_l)}{r_{kl}}u'(r_{kl})\right) + \sum_{l\neq k}\left(\frac{2}{r_{kl}}u'(r_{kl})+u''(r_{kl})\right) + \sum_{l\neq k}\sum_{n\neq k}\frac{(\boldsymbol{r}_k-\boldsymbol{r}_l)(\boldsymbol{r}_k-\boldsymbol{r}_n)}{r_{kl}r_{kn}}u'(r_{kl})u'(r_{kn}). \tag{D9}$$

It is now possible to express the local energy using equation 6 and D1. We start by defining

$$\frac{1}{\Psi_T(\boldsymbol{r})}\nabla_k^2\Psi_T(\boldsymbol{r}) = \underbrace{\frac{\nabla_k^2\phi(\boldsymbol{r}_k)}{\phi(\boldsymbol{r}_k)}}_{\textbf{Term 1}} + \underbrace{\frac{2\nabla_k\phi(\boldsymbol{r}_k)}{\phi(\boldsymbol{r}_k)}\left(\sum_{l\neq k}\frac{(\boldsymbol{r}_k-\boldsymbol{r}_l)}{r_{kl}}u'(r_{kl})\right)}_{\textbf{Term 2}} + \underbrace{\sum_{l\neq k}\left(\frac{2}{r_{kl}}u'(r_{kl})+u''(r_{kl})\right)}_{\textbf{Term 3}} + \underbrace{\sum_{l\neq k}\sum_{n\neq k}\frac{(\boldsymbol{r}_k-\boldsymbol{r}_l)(\boldsymbol{r}_k-\boldsymbol{r}_n)}{r_{kl}r_{kn}}u'(r_{kl})u'(r_{kn})}_{\textbf{Term 4}}. \tag{D10}$$

For **Term 1**, we obtain

$$\begin{aligned}\frac{\nabla_k^2\phi(\boldsymbol{r}_k)}{\phi(\boldsymbol{r}_k)} &= 4\alpha^2(x_k^2+y_k^2+\beta^2z^2) - 4\alpha - 2\alpha\beta \\ &= 2\alpha\left[2\alpha(x_k^2+y_k^2+\beta^2z^2) - 2 - \beta\right].\end{aligned} \tag{D11}$$

For **Term 2**, we get

$$\frac{2\nabla_k\phi(\boldsymbol{r}_k)}{\phi(\boldsymbol{r}_k)}\sum_{l\neq k}\frac{(\boldsymbol{r}_k-\boldsymbol{r}_l)}{r_{kl}}u'(r_{kl}) = -4\alpha(x_k,y_k,\beta z_k)\sum_{l\neq k}\frac{(\boldsymbol{r}_k-\boldsymbol{r}_l)}{r_{kl}}\frac{a}{r_{kl}(r_{kl-a})}.$$

For **Term 3** and **Term 4** we obtain

$$\sum_{j\neq k}\sum_{n\neq k}\frac{(\boldsymbol{r}_k-\boldsymbol{r}_j)(\boldsymbol{r}_k-\boldsymbol{r}_i)}{r_{kj}r_{ki}}u'(r_{kj})u'(r_{ki}) = \sum_{j\neq k}\sum_{i\neq k}\frac{(\boldsymbol{r}_k-\boldsymbol{r}_j)(\boldsymbol{r}_k-\boldsymbol{r}_i)}{r_{kj}r_{ki}}\frac{a}{r_{kj}(r_{kj-a})}\frac{a}{r_{ki}(r_{ki-a})} \tag{D12}$$

and,

$$\sum_{j\neq k}\left(\frac{2}{r_{kj}}u'(r_{kj})+u''(r_{kj})\right) = \sum_{j\neq k}\left(\frac{2}{r_{kj}}\frac{a}{r_{kj}(r_{kj}+a)}\frac{a(a-2r_{kj})}{r_{kj}^2(r_{kj}-a)^2}\right) \tag{D13}$$

The local energy can then be expressed as

$$E_L(\boldsymbol{r}) = \sum_i^N\Big[-\frac{\hbar^2}{2m}\Big(2\alpha(2\alpha(x_k^2+y_k^2+\beta^2z^2)-2-\beta) - 4\alpha(x_k,y_k,\beta z_k)\sum_{j\neq k}\frac{(\boldsymbol{r}_k-\boldsymbol{r}_j)}{r_{kj}}\frac{a}{r_{kj}(r_{kj-a})} \tag{D14}$$

$$\cdot\sum_{j\neq k}\sum_{i\neq k}\frac{(\boldsymbol{r}_k-\boldsymbol{r}_j)(\boldsymbol{r}_k-\boldsymbol{r}_i)}{r_{kj}r_{ki}}\frac{a}{r_{kj}(r_{kj-a})}\frac{a}{r_{ki}(r_{ki-a})} \tag{D15}$$

$$\cdot\sum_{j\neq k}\left(\frac{a(a-2r_{kj})}{r_{kj}^2(r_{kj}-a)^2}+\frac{2}{r_{kj}}\frac{a}{r_{kj}(r_{kj}-a)}\right)\Big) + V_{ext}(\boldsymbol{r}_k)\Big] \tag{D16}$$

$$+\sum_{i<j}^N V_{int}(\boldsymbol{r}_i,\boldsymbol{r}_j) \tag{D17}$$

Appendix E: Energy plots

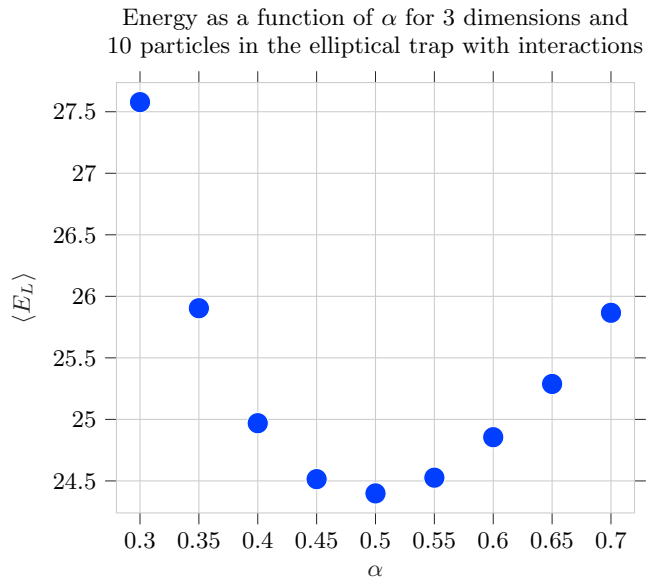

Figure 14. Energy as a function of the variational parameter, *lpha*, for 10 particles with interactions in 3 dimensions.

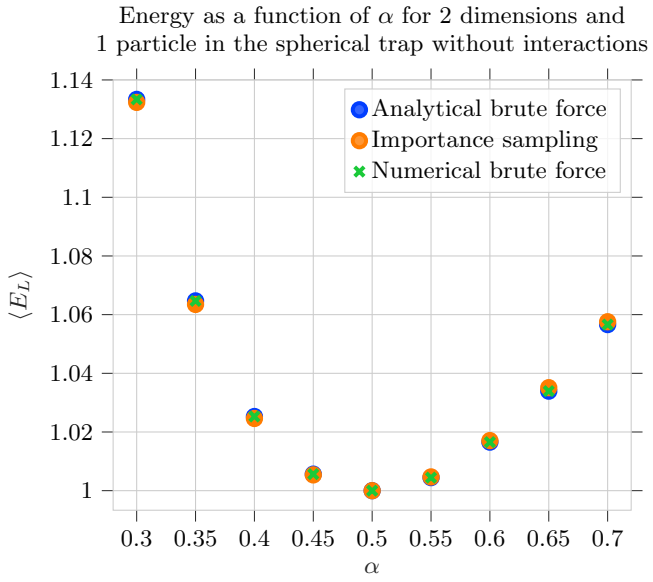

Figure 16. Energy as a function of the variational parameter, α, for 1 particle without interactions in 2 dimensions, for analytical and numerical brute force and importance sampling.

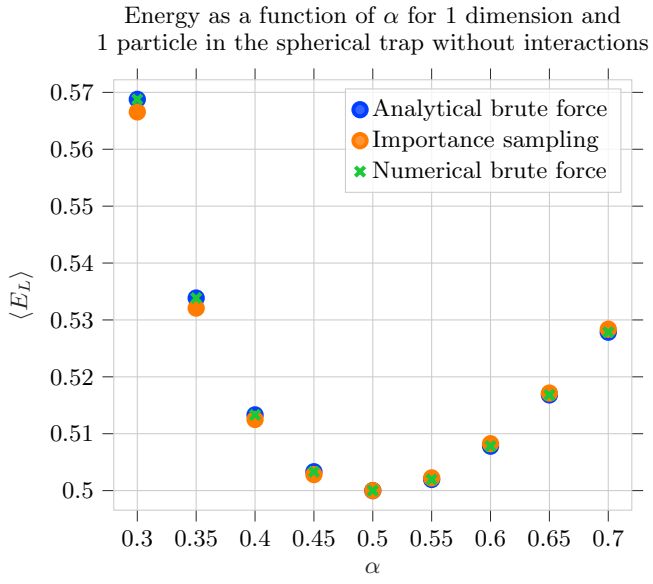

Figure 15. Energy as a function of the variational parameter, α, for 1 particle without interactions in 1 dimension, for analytical and numerical brute force and importance sampling.

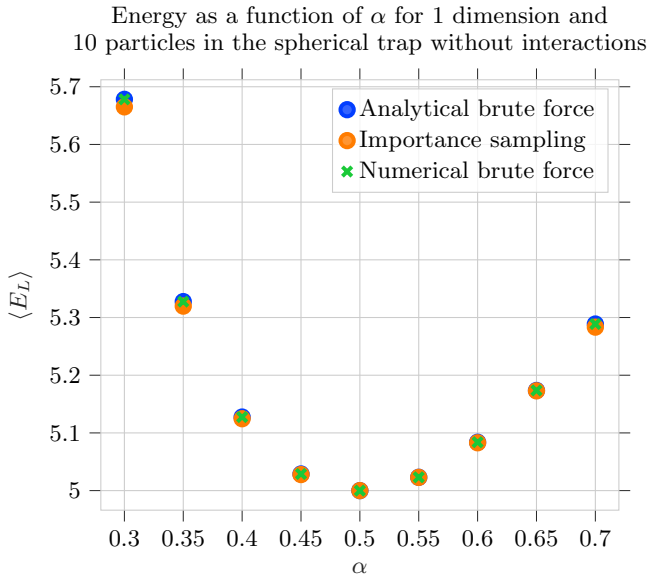

Figure 17. Energy as a function of the variational parameter, α, for 10 particles without interactions in 1 dimension, for analytical and numerical brute force and importance sampling.

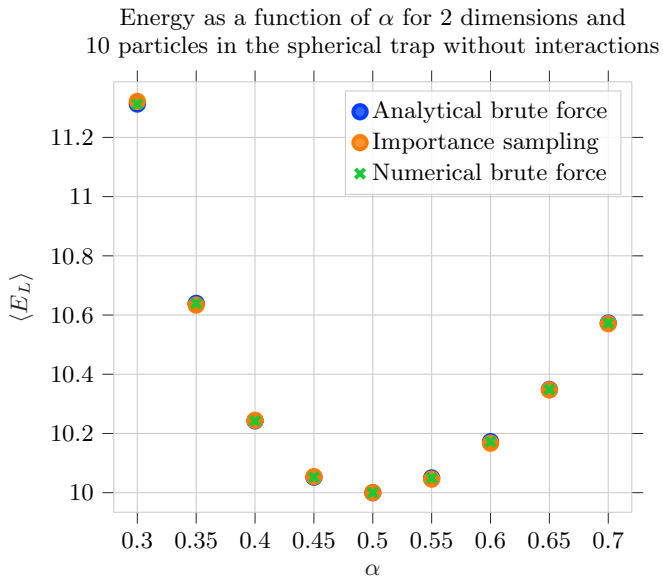

Figure 18. Energy as a function of the variational parameter, α, for 10 particles without interactions in 2 dimensions, for analytical and numerical brute force and importance sampling.

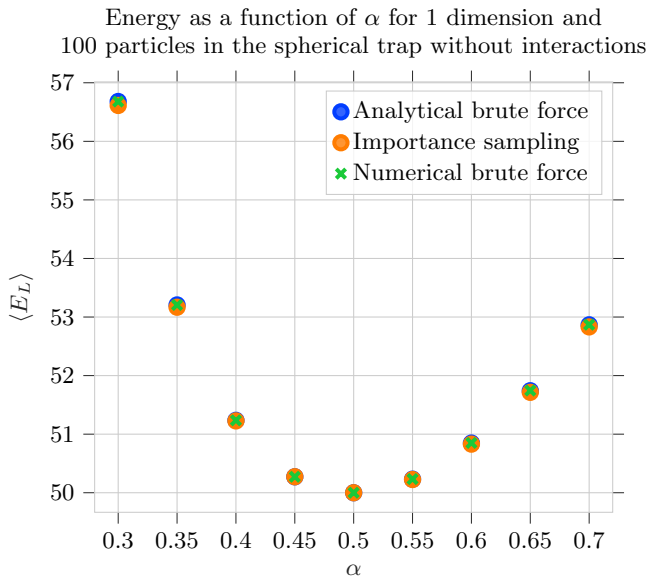

Figure 19. Energy as a function of the variational parameter, α, for 100 particles without interactions in 1 dimension, for analytical and numerical brute force and importance sampling.

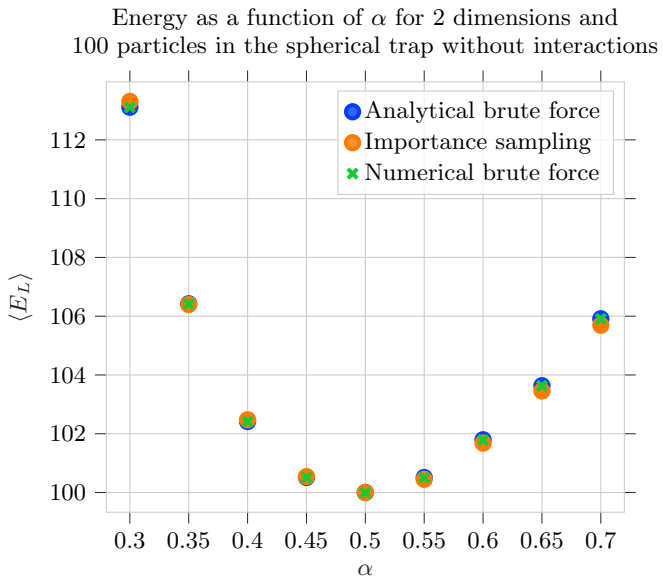

Figure 20. Energy as a function of the variational parameter, α, for 100 particles without interactions in 2 dimensions, for analytical and numerical brute force and importance sampling.

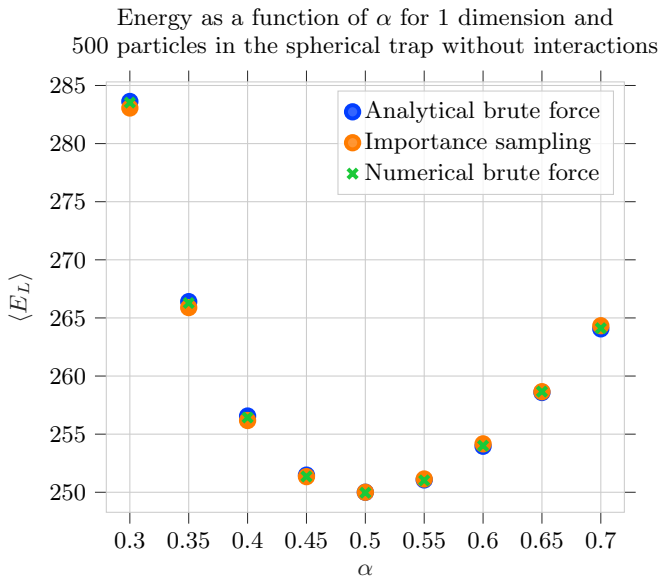

Figure 21. Energy as a function of the variational parameter, α, for 500 particles without interactions in 1 dimension, for analytical and numerical brute force and importance sampling.

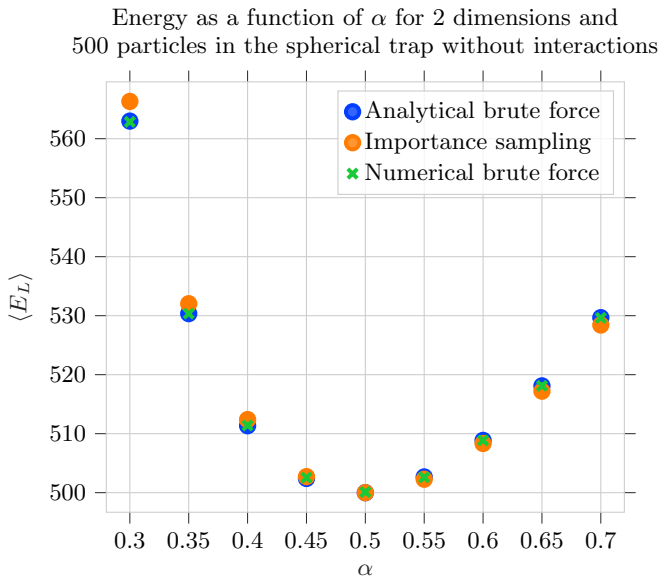

Figure 22. Energy as a function of the variational parameter, α, for 500 particles without interactions in 2 dimensions, for analytical and numerical brute force and importance sampling.